

1 **Detection of Darkships: Overview, Simulation** 2 **and Testing**

3 **VIOLONI GIANLUCA**¹

4 **gianluca.violoni@unitn.it*

5 **Abstract:** Detecting Dark Ships, vessels operating without active transponders, is a critical
6 task for maritime surveillance and security. These ships do not transmit their position via the
7 Automatic Identification System (AIS), making them invisible to conventional tracking methods.
8 This project aims to implement a customizable simulation framework and test algorithms for
9 the acoustic detection of dark ships using hydrophones, underwater microphones capable of
10 continuously monitoring ocean sounds.

11 **1. Introduction**

12 Maritime security faces a critical challenge in the detection and monitoring of "dark ships" -
13 vessels that deliberately disable or tamper with tracking systems to avoid detection by conventional
14 monitoring methods, including [Automatic Identification System \(AIS\)](#) data manipulation, position
15 spoofing, and strategic system shutdowns when entering sensitive or restricted areas. These
16 vessels represent a significant threat to maritime surveillance and security operations worldwide,
17 as they often engage in illicit activities such as illegal fishing, smuggling, sanctions evasion,
18 human trafficking, and unauthorized territorial intrusions. A notable example occurred in 2023,
19 [where tankers were found to be deceiving authorities by transmitting false positions while secretly](#)
20 [docking at terminals in Russia to transport oil to China, circumventing international sanctions.](#)
21 Current approaches to dark ship detection involve multiple technologies including satellite-based
22 monitoring (using optical imaging, Synthetic Aperture Radar, and radio frequency detection),
23 conventional radar systems, and various signal intelligence methods. However, these methods
24 face significant limitations including weather dependence, coverage gaps, latency issues, and
25 the high operational costs associated with continuous wide-area surveillance. Passive acoustic
26 monitoring offers distinct advantages as a complementary technology for the detection of dark
27 ships. Hydrophones - underwater microphones that detect acoustic signals - can continuously
28 monitor large maritime areas without requiring any cooperation from the vessels being observed.
29 The underwater acoustic channel presents unique challenges compared to terrestrial environments.
30 Sound propagation in water is affected by various factors including temperature gradients,
31 salinity variations, and depth-dependent changes in acoustic properties. Additionally, underwater
32 environments are characterized by complex ambient noise from both natural sources (marine life,
33 weather phenomena) and anthropogenic activities (other vessels, industrial operations).
34 This project focuses on implement and test algorithms for the passive acoustic detection of
35 dark ships using hydrophones, which capture underwater sound patterns generated by vessel
36 machinery, propellers, and hull interactions with the surrounding water.
37 To facilitate the design and evaluation of these detection algorithms, a configurable simulation
38 environment has been specifically developed. This environment enables the modeling of realistic
39 acoustic propagation conditions, various ship behaviors, and environmental factors such as
40 ambient noise and bathymetry. It also supports different hydrophone configurations, including
41 spatial layouts and sensitivity parameters, allowing the conduction of controlled experiments.

42 **2. Noise Factors Affecting AIS Transmission**

43 The Automatic Identification System (AIS) is a widely used method for tracking vessels, but
44 several factors can affect its reliability. The following are the main factors influencing AIS

45 transmission:

- 46 • **Equipment Issues:** Poor quality equipment or poor installation can cause gaps in AIS
47 transmissions.
- 48 • **Satellite Receiver Saturation:** In high-density areas, satellite receivers can become
49 saturated, leading to a loss of AIS data.
- 50 • **Signal Interference:** Environmental conditions such as weather and cloud coverage can
51 shield ships from detection.
- 52 • **Intentional Disabling:** Vessels may intentionally turn off their AIS transponders to avoid
53 observation, often linked to illegal activities.
- 54 • **AIS Message Collision:** In congested waters, signal collision and interference can cause
55 lost signals.
- 56 • **Small Vessel Regulations:** Smaller vessels may not be legally required to transmit AIS,
57 making their detection more difficult.
- 58 • **Spoofing:** Ships can transmit incorrect AIS information, including their identity or position,
59 often to deceive monitoring systems.

60 3. Potential Approaches for Detecting Dark Ships

61 The following approaches have been explored for identifying dark ships in maritime surveillance:

62 3.1. Spatial Statistical Models

63 These models help identify gaps in AIS transmission and calculate the probability that a gap
64 is due to intentional disabling. For example, a Generalized Additive Model (GAM) can model
65 space-time variations in AIS gaps to distinguish between intentional disabling and other issues.

66 3.2. Multi-Sensor Data Fusion

67 Combining data from various sources, such as satellite imagery and radio frequency sensors, can
68 help detect vessels that are not transmitting AIS. Common techniques include:

- 69 • **SAR (Synthetic Aperture Radar):** SAR does not require cooperation from ships and can
70 detect dark ships under all weather conditions.
- 71 • **Electro-Optical/Infrared (EO/IR) Imagery:** Optical imagery can detect ships regardless
72 of their AIS status but may be limited by weather conditions and darkness.
- 73 • **Radio Frequency (RF) Sensors:** RF sensors can detect vessels that have turned off their
74 AIS transponders.

75 3.3. Anomaly Detection Algorithms

76 Anomaly detection techniques, such as trajectory analysis and machine learning models, can help
77 identify suspicious vessel behavior. Common methods include:

- 78 • **Trajectory Analysis:** Using machine learning to detect deviations from normal vessel
79 behavior, based on kinematic data such as speed and course.
- 80 • **Clustering Techniques:** Identifying abnormal data by comparing AIS data with kinematic-
81 based estimations.

- 82 • **Machine Learning:** Self-supervised deep learning models can predict whether an AIS
83 message should be received, flagging deviations as suspicious.
- 84 • **Pattern-of-Life (PoL) Analysis:** This method analyzes vessel behavior patterns over time
85 to detect unusual activities.

86 3.4. AIS Signal Analysis

87 Several methods can analyze AIS signal strength and patterns to identify intentional on/off
88 switching:

- 89 • **Received Signal Strength Indicator (RSSI):** Analyzing RSSI at AIS base stations can
90 help detect intentional AIS transponder switching.
- 91 • **Channel Memory:** Hidden Markov Models (HMMs) can detect switching patterns by
92 analyzing signal transmission behavior.

93 3.5. Cross-Referenced Data

94 Combining AIS data with other sensor information, such as radar data, can enhance detection
95 reliability:

- 96 • **Radar Data:** Radar can provide real-time vessel trajectories, which can be cross-referenced
97 with AIS data to identify spoofing or missing transmissions.

98 4. Specific Detection Techniques

99 There are several specific techniques used to detect dark ships, including advanced machine
100 learning algorithms and image processing methods:

101 4.1. YOLO (You Only Look Once) and SAHI

102 Combining YOLO with the SAHI module improves the detection of small ships in large SAR
103 images. SAHI works by slicing large images into smaller regions, making small targets more
104 prominent.

105 4.2. CFAR (Constant False Alarm Rate) Detectors

106 CFAR algorithms are used to detect ships in SAR images by modeling background clutter. An
107 improved version, AIS-RCFAR, uses AIS data to trim outliers and improve detection accuracy.

108 4.3. Dead Reckoning (DR)

109 Comparing a GNSS position with a position calculated using DR can help detect GNSS spoof
110 attacks and identify vessels that do not transmit AIS.

111 5. Challenges and Considerations

112 Detecting dark ships involves addressing several challenges, including:

- 113 • **False Positives vs. False Negatives:** Balancing the risk of incorrectly identifying a normal
114 vessel as a dark ship (false positives) versus missing a dark ship (false negatives) is crucial
115 for accurate detection.
- 116 • **Small Ship Detection:** Smaller vessels are often missed in both imagery and AIS data,
117 making their detection more difficult.

- 118 • **Data Quality:** AIS data can be unreliable, with errors in vessel information such as size
119 and type.
- 120 • **Adaptive Behavior:** Malicious actors may adjust their behavior to avoid detection,
121 requiring adaptable detection systems.
- 122 • **Privacy Concerns:** AIS surveillance raises concerns about privacy, as it allows continuous
123 tracking of ships and their activities.
- 124 • **Standardized Datasets:** A lack of labeled datasets with ground truth information makes it
125 difficult to compare and validate different detection methods.

126 6. Passive Acoustic Monitoring with Hydrophones

127 Hydrophones are underwater microphones that capture acoustic signals in the marine environment.
128 They enable passive acoustic monitoring by recording ambient noise, ship engine sounds, and
129 other underwater activities without the need for active emissions. In the context of dark ship
130 detection, hydrophones offer a complementary source of information to satellite and radar-based
131 systems, particularly when AIS signals are missing or intentionally disabled.

132 6.1. Advantages of Using Hydrophones

- 133 • **Passive Detection:** No active emission; stealthy and non-intrusive.
- 134 • **All-Weather Capability:** Unaffected by atmospheric or sea surface conditions.
- 135 • **Continuous Monitoring:** Hydrophones can record data 24/7 without interruption.
- 136 • **Long-Range Detection:** Low-frequency sounds can travel long distances underwater,
137 allowing early detection of approaching vessels.

138 6.2. Challenges in Hydrophone-Based Detection

- 139 • **Ambient Noise:** Natural sounds (e.g., waves, rain, marine fauna) and anthropogenic noise
140 (e.g., other ships) can mask vessel signals.
- 141 • **Multipath Propagation:** Acoustic signals may reflect off the sea surface or seabed,
142 complicating signal analysis.
- 143 • **Source Localization:** Estimating the exact position of a vessel and differentiating between
144 vessel types requires multiple hydrophones and complex algorithms.

145 7. Simulation Framework

146 The developed simulation framework is organized into three distinct stages, each addressing a
147 specific phase of the dark ship detection pipeline:

- 148 • **Simulation Module** — This component generates a dynamic virtual maritime environment.
149 It models ship trajectories, environmental conditions, and the propagation of underwater
150 acoustic signals. As the simulation progresses, relevant data such as ship positions,
151 hydrophone observations, and acoustic pressure fields are computed and stored in an output
152 file. This file serves as the ground truth dataset for subsequent processing stages.
- 153 • **Tracking Module** — In this stage, the data produced by the simulation module is
154 processed by acoustic detection and tracking algorithms. The tracking module analyzes
155 the hydrophone observations to infer ship positions and behaviors over time. The results,
156 including both raw observations and tracking outputs, are compiled into a structured output
157 file used for visualization and further evaluation.

158 • **Visualization and Analysis Tool** — This component processes the output produced by
 159 the tracking module and generates a variety of informative plots and statistics. It allows
 160 users to visualize ship trajectories, hydrophone positions, detection events, and error
 161 metrics through time-series plots, spatial maps, and summary charts. The tool supports
 162 in-depth exploration and evaluation of the tracking algorithms in a flexible and scriptable
 163 environment, making it ideal for research and prototyping purposes.

164 This modular architecture allows for flexibility in testing different algorithmic approaches,
 165 simulation scenarios, and visualization strategies. It also supports reproducibility and systematic
 166 evaluation by separating data generation from inference and rendering.

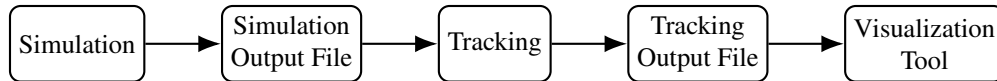


Fig. 1. Simulation-to-Visualization processing pipeline.

167 7.1. Configuration

168 The simulation is initialized through a YAML configuration file, which defines all parameters
 169 required to generate the environment, simulate ship movements, and specify sensor behavior.
 170 The main configuration sections are as follows:

171 • **Paths and general configuration:**

- 172 – `output_path`: the output path where the simulation will store its results.
- 173 – `name`: identification name for the simulation.

174 • **Environment parameters:**

- 175 – `area`: the geographic region to be simulated, defined as `[lat_min, lat_max,`
 176 `lon_min, lon_max]`.
- 177 – `bathymetry_path`: the path to a NetCDF file containing bathymetric data, which
 178 is used to simulate realistic underwater sound propagation influenced by seabed
 179 topography.
- 180 – `toa_variance`: array of variance values for the time of arrival, used to simulate
 181 different levels of noise in time measurements.

182 • **Hydrophone configuration:**

- 183 – `hydrophones`: a list of manually placed hydrophones, each defined by geographic
 184 coordinates and depth.
- 185 – `noise_level`: the ambient underwater noise level, expressed in dB re 1 μ Pa,
 186 which affects the detectability of ships.
- 187 – `num_random`: the number of additional hydrophones to be generated randomly.
- 188 – `max_range_range`: range for the maximum detection range of randomly gener-
 189 ated hydrophones, in km.
- 190 – `depth_range`: depth interval for randomly generated hydrophones, in meters.

191 • **Ship configuration:**

- 192 – `ais_ships`: manually defined ships with active AIS, each specified by position,
 193 speed, depth, and heading.

- 194 - dark_ships: manually defined "dark" ships, which do not transmit AIS, defined
- 195 with the same attributes.
- 196 - num_random_ais_ships: number of AIS ships to be generated randomly.
- 197 - num_random_dark_ships: number of dark ships to be generated randomly.
- 198 - speed_range: speed interval for random ship generation, in knots.
- 199 - depth_range: depth interval for random ship generation, in meters.

200 An example of configuration file is reported below.

```

1  output_path: "/Users/gean/Documents/Unitn/Thesis/darkships_detection/output"
2  name: "test"
3
4  environment:
5      area: [10, 12, 83.5, 85.5] # lat_min, lat_max, long_min, long_max
6      bathymetry_path: "./bathymetry/bathymetry_sample.nc"
7      toa_variance: [1.0e-5, 1.0e-4, 1.0e-3, 1.0e-2, 1.0e-1, 1.0]
8
9  hydrophones_config:
10     # DATA FOR MANUAL HYDROPHONES GENERATION
11     hydrophones:
12         - coordinates: [11.0, 84.0]      # Hydrophone 1
13           depth: 20                      # [m]
14         - coordinates: [11.03, 84.0]     # Hydrophone 2
15           depth: 20                      # [m]
16         - coordinates: [11.03, 84.03]    # Hydrophone 3
17           depth: 20                      # [m]
18         - coordinates: [11.0, 84.03]     # Hydrophone 4
19           depth: 20                      # [m]
20     noise_level: 2.0                    # [dB re 1 µPa]
21
22     # DATA FOR RANDOM HYDROPHONES GENERATION
23     num_random: 0                       # Generate random hydrophones
24     max_range_range: [30, 50]           # [km]
25     depth_range: [0, 35]                # [m]
26
27  ships_config:
28     dark_ships:                          # Manual dark ships
29         - coordinates: [11.032, 84.015]  # Dark Ship 1
30           speed: 10                      # kt
31           depth: 20                      # [m]
32           heading: 180                   # [°]
33
34     # DATA FOR RANDOM SHIPS GENERATION
35     num_random_ais_ships: 0              # Generate random ais ships
36     num_random_dark_ships: 0            # Generate random dark ships
37     speed_range: [5, 20]                 # [kt]
38     depth_range: [0, 25]                 # [m]
39

```

201 This configuration approach provides a high degree of flexibility, allowing for both precise
202 control through manual definition and broad scenario testing through random generation. The
203 structure ensures reproducibility and scalability for experiments that involve different maritime
204 scenarios and detection strategies.

205 7.2. Underwater Sound Propagation

206 To simulate acoustic propagation and model how sound attenuates with distance and depth, the
207 simulation uses the [Bellhop acoustic ray-tracing model](#). Bellhop takes into account bathymetry
208 and other environmental parameters to calculate the *transmission loss* and *time of arrival* between
209 each ship and hydrophone pair. This allows the system to estimate the *received sound pressure*
210 *level* in each hydrophone, given the level and position of the source of the ship.
211 The simulation runs with a range of TOA variance values to analyze how measurement errors
212 impact the detection and localization accuracy under different noise conditions, providing a more
213 realistic assessment of the system's performance in real-world environments.

214
215 The simulated readings at the hydrophones are influenced by the following.

- 216 • The number and proximity of vessels (both AIS and dark).
- 217 • Their source levels.
- 218 • Environmental factors such as depth, shape of the seabed, and background noise.

219 8. DARKSHIP TRACKING APPROACHES USING HYDROPHONES

220 8.1. Weighted Centroid Localization (WCL)

221 Weighted Centroid Localization is a geometric technique for source localization based on the
222 assumption that signal strength (or in this case, pressure differential) diminishes with distance from
223 the source. Each hydrophone contributes to the estimated position of the source proportionally to
224 the measured acoustic intensity.

225 Given a set of N hydrophones with coordinates (ϕ_i, λ_i) and corresponding measured pressure
226 differences Δ_i , the estimated position $(\hat{\phi}, \hat{\lambda})$ is computed as:

$$\hat{\phi} = \frac{\sum_{i=1}^N \phi_i \cdot \Delta_i}{\sum_{i=1}^N \Delta_i} \quad (1)$$

$$\hat{\lambda} = \frac{\sum_{i=1}^N \lambda_i \cdot \Delta_i}{\sum_{i=1}^N \Delta_i} \quad (2)$$

227 This estimation can be implemented as follows in Python:

```
21 def weighted_centroid_localize(hydrophones: list[Hydrophone]):
22     deltas = [h.compute_pressure_delta() for h in hydrophones]
23     delta_tot = sum(deltas)
24
25     if delta_tot == 0:
26         return (0.0, 0.0)
27
28     weighted_lat = sum(
29         h.coord.latitude * d for h, d in zip(hydrophones, deltas)
30     ) / delta_tot # as (1)
31
32     weighted_lon = sum(
33         h.coord.longitude * d for h, d in zip(hydrophones, deltas)
34     ) / delta_tot # as (2)
35
36     return weighted_lat, weighted_lon
```

228 In this implementation, lines [8–10] and [12–14] respectively compute the latitude and
229 longitude of the estimated source position by applying equations (1) and (2).

230 **Advantages.** The main advantages of WCL are its simplicity and speed, making it suitable
 231 for real-time applications or as an initialization step for more complex tracking algorithms (e.g.,
 232 particle filters).

233 **Limitations.** The reliability of Weighted Centroid Localization significantly decreases in
 234 complex underwater environments where signal propagation is strongly affected by factors such
 235 as bathymetry, thermoclines, seabed composition, and multipath reflections. In such conditions,
 236 the measured pressure deltas are no longer directly correlated with distance to the source, violating
 237 the core assumption of this method. As a result, the estimated position may become highly
 238 inaccurate or biased. Therefore, WCL is best suited for relatively homogeneous environments or
 239 as an initial estimate to be refined by more robust methods.

240 8.2. Time Difference of Arrival (TDOA) Localization

241 Time Difference of Arrival (TDOA) is a well-established technique for passive source localization
 242 based on the differences in signal arrival times across a set of spatially distributed sensors. In this
 243 context, hydrophones record the acoustic pressure waveform emitted by a ship, and the algorithm
 244 estimates the source's position by solving a system derived from the time delays between sensors.

245 The implementation follows the closed-form localization algorithm described in [1], which
 246 assumes that the positions of the hydrophones and the speed of sound in water v are known.
 247 One hydrophone (typically the first) is used as a reference. For each other hydrophone, the time
 248 difference $\tau_i = t_i - t_1$ is used to build a linear system based on the following equations:

$$A_i = \frac{1}{v\tau_i}(-2x_1 + 2x_i) - \frac{1}{v\tau_2}(-2x_1 + 2x_2) \quad (3)$$

$$B_i = \frac{1}{v\tau_i}(-2y_1 + 2y_i) - \frac{1}{v\tau_2}(-2y_1 + 2y_2) \quad (4)$$

$$D_i = v(\tau_i - \tau_2) + \frac{1}{v\tau_i}(x_1^2 + y_1^2 - x_i^2 - y_i^2) - \frac{1}{v\tau_2}(x_1^2 + y_1^2 - x_2^2 - y_2^2) \quad (5)$$

251 By stacking the coefficients A_i , B_i and D_i into matrices, the final source position (x, y) in
 252 UTM coordinates is estimated by solving the system:

$$\begin{bmatrix} A_3 & B_3 \\ \vdots & \vdots \\ A_i & B_i \end{bmatrix} \cdot \begin{bmatrix} x \\ y \end{bmatrix} = \begin{bmatrix} -D_3 \\ \vdots \\ -D_i \end{bmatrix} \quad (6)$$

253 using the Moore-Penrose pseudoinverse.

254 The algorithm is implemented in Python as follows:

```

1  def tdoa_localize(self, v_water=None):
2      """
3      Implement TDOA localization using the algorithm from the paper [1].
4      Returns the estimated position in geographic coordinates (lat, lon).
5      """
6      # Use class-level sound speed if none provided
7      if v_water is None:
8          v_water = self.v
9
10     s = self.get_utm_coords()
11

```



```

12     # First hydrophone (reference)
13     s1 = s[0]
14     x1, y1 = s1
15
16     # Second hydrophone
17     if len(s) < 2:
18         raise ValueError("Need at least two hydrophones for TDOA")
19
20     s2 = s[1]
21     x2, y2 = s2
22
23     # Calculate time differences (TDOA)
24     # Reference time is from first hydrophone
25     t1 = self.hydrophones[0].observed_pressure[-1]["toa"]
26
27     # Pre-calculate tau_2 (time difference between second and first hydrophone)
28     tau_2 = self.hydrophones[1].observed_pressure[-1]["toa"] - t1
29
30     A = []
31     D = []
32
33     # Process hydrophones from index 2 onwards
34     for i in range(2, len(self.hydrophones)):
35         xi, yi = s[i]
36
37         # Calculate time difference between current hydrophone and reference
38         tau_i = self.hydrophones[i].observed_pressure[-1]["toa"] - t1
39
40         # Guard against division by zero
41         if abs(tau_i) < 1e-10 or abs(tau_2) < 1e-10:
42             continue
43
44         # Computing A_i, B_i, D_i as per equations (3)-(5)
45         Ai = (1 / (v_water * tau_i)) * (-2 * x1 + 2 * xi) - (
46             1 / (v_water * tau_2)
47         ) * (-2 * x1 + 2 * x2)
48
49         Bi = (1 / (v_water * tau_i)) * (-2 * y1 + 2 * yi) - (
50             1 / (v_water * tau_2)
51         ) * (-2 * y1 + 2 * y2)
52
53         Di = (
54             v_water * tau_i
55             - v_water * tau_2
56             + (1 / (v_water * tau_i)) * (x1**2 + y1**2 - xi**2 - yi**2)
57             - (1 / (v_water * tau_2)) * (x1**2 + y1**2 - x2**2 - y2**2)
58         )
59
60         A.append([Ai, Bi])
61         D.append(-Di)
62
63     # Check if we have enough measurements to compute position
64     if len(A) == 0:
65         raise ValueError("Not enough valid measurements to compute position")
66

```

```

67     # Convert to numpy arrays
68     A = np.array(A)
69     D = np.array(D)
70
71     # Moore-Penrose pseudoinverse to solve A @ [x, y] = D as in equation (6)
72     position_utm = np.linalg.pinv(A) @ D
73
74     # Convert UTM coordinates back to geographic coordinates
75     lon, lat = self.utm_to_geo(position_utm[0], position_utm[1])
76
77     return (lat, lon)

```

Lines [44–61] correspond to equations (3), (4) and (5), while line [72] solves the linear system (6).

Advantages. TDOA offers high localization accuracy when time-of-arrival estimates are precise and hydrophones are well-distributed spatially. It does not assume a simple attenuation model and instead leverages time synchronization, making it more robust in complex acoustic environments.

Limitations. The accuracy of this method strongly depends on synchronization between hydrophones and the precision of time-of-arrival estimates. Environmental noise, signal reflections, and multipath propagation can distort TOA measurements, introducing error. Moreover, the algorithm requires at least three hydrophones (with two providing valid TOA deltas), which may not always be available.

8.3. TDOA Acoustical Location Based on Majorization-Minimization Optimization (T-MM)

The T-MM localization algorithm employs an iterative optimization approach based on the Majorization-Minimization framework to solve the non-convex TDOA localization problem. This method aims to find a robust estimate of the source position by iteratively minimizing a cost function derived from the squared differences between measured and predicted distances.

Initial Point Selection (Algorithm 2) Finding a suitable initial point is crucial for the convergence of the MM algorithm. Following Algorithm 2 from [1], the initial point \mathbf{x}_0 is selected by minimizing the cost function

$$f(\mathbf{x}) = \sum_{i=1}^N (\|\mathbf{x} - \mathbf{s}_i\| - d_i)^2, \quad (7)$$

where \mathbf{s}_i are the known hydrophone coordinates in UTM and the distances d_i represent the difference in distance between the acoustic source and each hydrophone relative to a reference hydrophone (typically the first one). These values are derived from the Time Difference of Arrival (TDOA) measurements.

Specifically, given the measured time of arrival t_i at each hydrophone i , and t_1 at the reference hydrophone, the time differences are calculated as:

$$\text{TDOA}_i = t_i - t_1$$

Multiplying these time differences by the speed of sound in water v converts them into distance differences:

$$d_i = \text{TDOA}_i \times v = (t_i - t_1) \times v$$

The procedure consists of:

- 283 1. Evaluating $f(\mathbf{s}_k)$ for each hydrophone position \mathbf{s}_k and selecting the k that minimizes it
284 (equation (8) in [1]).
- 285 2. Computing the gradient $\mathbf{g}_k(\mathbf{s}_k)$ (as in equation (29) in [1]) to determine the search
286 direction.
- 287 3. Performing a backtracking line search along this direction to find an optimal step size t ,
288 ensuring $f(\mathbf{s}_k + t\mathbf{v}_0) < f(\mathbf{s}_k)$.

289 This process returns the initial estimate \mathbf{x}_0 used in the iterative MM algorithm.

```

1  def _find_initial_point(self):
2      """
3      Algorithm 2 from the paper: Find an optimal initial point for the MM algorithm
4      Reference: Minimizing equation (7)
5      """
6
7      s = self.get_utm_coords()
8      distances = self._compute_distances()
9
10     # Step 1: Find index k for which f(s_k) is minimum
11     # Equation (8) from paper [1]: f(x) = sum_i (||x - s_i|| - d_i)^2
12     min_f_val = float("inf")
13     min_idx = 0
14
15     for k in range(len(s)):
16         f_val = 0
17         for i in range(len(s)):
18             # d_i is distances[i], ||s_k - s_i|| is Euclidean distance
19             dist = np.linalg.norm(s[k] - s[i])
20             f_val += (dist - distances[i]) ** 2
21
22         if f_val < min_f_val:
23             min_f_val = f_val
24             min_idx = k
25
26     # Step 2: Calculate gradient g_k(s_k)
27     # Equation (29) from paper [1]
28     g_k = np.zeros(2)
29     for i in range(len(s)):
30         if i != min_idx:
31             s_k_minus_s_i = s[min_idx] - s[i]
32             dist = np.linalg.norm(s_k_minus_s_i)
33
34             if dist > 1e-10: # Avoid division by zero
35                 g_k += 2 * (dist - distances[i]) * s_k_minus_s_i / dist
36
37     # Step 3: Determine direction vector v_0
38     # Use equation in Algorithm 2 from paper [1]
39     if np.linalg.norm(g_k) > 1e-10:
40         v_0 = -g_k / np.linalg.norm(g_k)
41     else:
42         # If gradient is zero or very small, use arbitrary unit vector
43         v_0 = np.array([1.0, 0.0])
44

```

```

45     # Step 4: Search for step size t with binary search
46     t = 1.0 # Initial value
47     x_0 = s[min_idx] + t * v_0
48
49     # Function to evaluate f(x) at position x
50     def evaluate_f(x):
51         f_val = 0
52         for i in range(len(s)):
53             dist = np.linalg.norm(x - s[i])
54             f_val += (dist - distances[i]) ** 2
55         return f_val
56
57     # f(s_k) at starting point
58     f_s_k = evaluate_f(s[min_idx])
59
60     # Binary search to find optimal t
61     max_iterations = 20
62     for iter in range(max_iterations):
63         x_0 = s[min_idx] + t * v_0
64         f_x0 = evaluate_f(x_0)
65
66         # Check condition in Algorithm 2: f(s_k + t*v_0) < f(s_k)
67         if f_x0 < f_s_k:
68             break
69
70         # Reduce t and try again
71         t /= 2.0
72
73         # If t becomes too small, use s_k as initial point
74         if t < 1e-8:
75             x_0 = s[min_idx]
76             break
77
78     # If we reach maximum iterations without finding a valid point
79     if iter == max_iterations - 1:
80         x_0 = s[min_idx]
81
82     return x_0

```

290 **Iterative Localization (Algorithm 3)** Algorithm 3 applies the MM iterative scheme to refine
291 the source position estimate. Starting from \mathbf{x}_0 , the algorithm updates the estimate using the rule
292 (equation (26) in [1]):

$$\mathbf{x}^{(r+1)} = \frac{\sum_{i=1}^N \left(\mathbf{s}_i + d_i \frac{\mathbf{x}^{(r)} - \mathbf{s}_i}{\|\mathbf{x}^{(r)} - \mathbf{s}_i\|} \right)}{\sum_{i=1}^N 1}, \quad (8)$$

293 where r denotes the iteration index.

294 The iterations continue until convergence criteria are met, specifically when the change in
295 position between iterations falls below a defined tolerance, or the maximum number of iterations
296 is reached.

```

1  def tmm_localize(self, max_iterations=100, tolerance=1e-8):
2      """

```

```

3      Algorithm 3 from the paper: T-MM underwater acoustic-based location algorithm.
4      Reference: equations (28)-(29)
5      """
6
7      s = self.get_utm_coords()
8      tdoa_diffs = self._compute_distances() #  $d_i = v_{water} * \tau_i (d_i - d_1)$ 
9
10     # Step 1: Initial x est
11     x_init = self._find_initial_point()
12
13     dl_init = np.linalg.norm(x_init - s[0])
14     di_fixed = [dl_init + tdoa_diffs[i] for i in range(len(s))]
15
16     def compute_objective(x):
17         return sum(
18             (np.linalg.norm(x - s[i]) - di_fixed[i]) ** 2 for i in range(len(s))
19         )
20
21     # Step 3: MM iterations with fixed  $d_i$ 
22     x_current = x_init.copy()
23     for _ in range(max_iterations):
24         x_prev = x_current.copy()
25
26         numerator = np.zeros(2)
27         denominator = 0
28         for i in range(len(s)):
29             direction = x_current - s[i]
30             norm_dir = np.linalg.norm(direction)
31             if norm_dir < 1e-10:
32                 continue
33             numerator += s[i] + di_fixed[i] * (direction / norm_dir)
34             denominator += 1
35         x_current = numerator / denominator # Eq. (26)
36
37         if np.linalg.norm(x_current - x_prev) < tolerance:
38             break
39
40     lon, lat = self.utm_to_geo(x_current[0], x_current[1])
41     return lat, lon

```

297 **Advantages.** The main advantage of the T-MM algorithm is its robustness in realistic scenarios
298 where time-of-arrival (TOA) data are corrupted by noise and environmental effects. In such
299 conditions, the T-MM algorithm tends to outperform classical TDOA methods by providing more
300 accurate and stable localization results. Its iterative majorization-minimization framework also
301 ensures monotonic convergence and improved stability through the initial point selection step.

302 **Limitations.** The method requires knowledge of accurate distance measurements and may be
303 computationally heavier than closed-form solutions. Convergence to a global optimum is not
304 guaranteed if the initial point is poorly chosen.

305 8.4. Squared Range-based Least Squares (SR-LS)

306 The Squared Range-based Least Squares (SR-LS) approach offers an alternative methodology
307 for underwater acoustic source localization. Unlike standard TDOA methods, SR-LS optimizes

308 squared range measurements between the source and sensors, as proposed in [2].

309 The SR-LS method formulates the localization problem as:

$$(SR-LS) : \min_{\mathbf{x}} \sum_{i=1}^m \left(\|\mathbf{x} - \mathbf{a}_i\|^2 - r_i^2 \right)^2 \quad (9)$$

310 where \mathbf{x} is the source coordinate vector to be estimated, \mathbf{a}_i are the known coordinates of the
311 i -th hydrophone, and r_i is the measured distance from the i -th hydrophone to the source.

312 Although this optimization problem is non-convex, it can be solved globally and efficiently.
313 The solution approach transforms the problem into a Generalized Trust Region Subproblem
314 (GTRS), which involves minimizing a quadratic function subject to a single quadratic constraint:

$$\min_{\mathbf{y} \in \mathbb{R}^{n+1}} \{ \|\mathbf{A}\mathbf{y} - \mathbf{b}\|^2 : \mathbf{y}^T \mathbf{D}\mathbf{y} + 2\mathbf{f}^T \mathbf{y} = 0 \} \quad (10)$$

315 The optimal solution is given by $\hat{\mathbf{y}}(\lambda) = (\mathbf{A}^T \mathbf{A} + \lambda \mathbf{D})^{-1} (\mathbf{A}^T \mathbf{b} - \lambda \mathbf{f})$, where λ is the unique
316 solution of a secular equation that can be efficiently solved using bisection methods.

317 One key advantage of SR-LS is that, despite being non-convex, it provides an exact global
318 solution rather than an approximation. This contrasts with other approaches that rely on
319 relaxation techniques or discarding constraints, which often lead to suboptimal results. Numerical
320 experiments have shown that SR-LS significantly outperforms approximate methods such as
321 unconstrained squared-range based LS (USR-LS) and semidefinite relaxation (SDR) approaches,
322 especially in high-noise scenarios.

323 It's worth noting that the SR-LS approach is suboptimal in the maximum likelihood sense
324 when compared to range-based least squares (R-LS) formulations, particularly under Gaussian
325 noise assumptions. This is because the covariance matrix of squared errors in the squared range
326 domain is not proportional to the identity matrix. However, the ability to compute the exact global
327 solution of SR-LS efficiently makes it particularly attractive for underwater acoustic localization
328 applications.

329 This method is implemented in Python as follows:

```

1  def _construct_matrix_A(self):
2      s = self.get_utm_coords()
3      m = len(s)
4
5      A = []
6
7      # compute matrix A as (17) in [2]
8      for i in range(m):
9          A.append([s[i][0] * (-2), s[i][1] * (-2), 1])
10
11     A = np.array(A)
12
13     return A
14
15  def _construct_vector_b(self):
16      # compute vector b as (17) in [2]
17      coords = np.array(self.get_utm_coords())
18      r_squared = np.array(
19          [
20              (hydro.observed_pressure[-1]["toa"] * self.v) ** 2
21              for hydro in self.hydrophones
22          ]

```

```

23     )
24
25     a_norm_squared = np.sum(coords**2, axis=1)
26
27     return r_squared - a_norm_squared
28
29     def _construct_matrix_D(self):
30         # compute matrix D as (18) in [2]
31         s = self.get_utm_coords()
32         n = len(s[0])
33
34         D = np.zeros((n + 1, n + 1))
35
36         D[:n, :n] = np.eye(n)
37
38         return D
39
40     def _construct_vector_f(self):
41         # compute vector f as (18) in [2]
42
43         n = len(self.get_utm_coords()[0])
44         f = np.zeros(n + 1)
45         f[n] = -0.5
46
47         return f
48
49     def sr_ls_localize(self):
50         # Compute matrix A and vector b as (17) in [2]
51         A = self._construct_matrix_A()
52         b = self._construct_vector_b()
53
54         # Compute matrix D and vector f as (18) in [2]
55         D = self._construct_matrix_D()
56         f = self._construct_vector_f()
57
58         # Find optimal lambda as (24) in [2]
59         lambda_opt = self.find_optimal_lambda(A, b, D, f)
60
61         # Compute position estimation
62         source_position = self.calculate_position_estimate(lambda_opt, A, b, D, f)
63
64         # return coord in (lat, lon) format
65         lon, lat = self.utm_to_geo(source_position[0], source_position[1])
66         return lat, lon
67
68     def determine_lambda_interval(self, A, D):
69         # Compute lower bound for interval I for lambda as eq. (26) in [2]
70
71         # Compute  $A^T A$ 
72         ATA = A.T @ A
73
74         # Compute lowest eigenvalue
75         eigvals = scipy.linalg.eigvals(D, ATA)
76         lambda_min = min(abs(eigvals))
77

```

```

78     # Compute lower bound as (26) in [2]
79     lower_bound = -1 / lambda_min + 1e-10
80
81     return lower_bound
82
83 def phi_function(self, lambda_val, A, b, D, f):
84     # Compute value of () as eq. (25) in [2]
85
86     try:
87         # Compute A^T A + D
88         ATA_plus_lambda_D = A.T @ A + lambda_val * D
89
90         # Compute A^T b - f
91         ATb_minus_lambda_f = A.T @ b - lambda_val * f
92
93         # Compute  $\hat{y}() = (A^T A + D)^{-1} (A^T b - f)$ 
94         y_lambda = np.linalg.solve(ATA_plus_lambda_D, ATb_minus_lambda_f)
95
96         # Compute  $() = \hat{y}()^T D \hat{y}() + 2f^T \hat{y}()$ 
97         phi_val = y_lambda.T @ D @ y_lambda + 2 * f.T @ y_lambda
98
99         return phi_val
100    except np.linalg.LinAlgError:
101        return float("inf")
102
103 def find_optimal_lambda(self, A, b, D, f):
104     # Find optimal value of lambda as () = 0, eq. (24) in [2]
105
106     lower_bound = self.determine_lambda_interval(A, D)
107     upper_bound = 1e6
108
109     def phi_for_bisect(lambda_val):
110         return self.phi_function(lambda_val, A, b, D, f)
111
112     lower_val = phi_for_bisect(lower_bound)
113     upper_val = phi_for_bisect(upper_bound)
114
115     if lower_val * upper_val > 0:
116         if abs(lower_val) < abs(upper_val):
117             return lower_bound
118         else:
119             return upper_bound
120
121     optimal_lambda = scipy.optimize.bisect(
122         phi_for_bisect, lower_bound, upper_bound, rtol=1e-6
123     )
124
125     return optimal_lambda
126
127 def calculate_position_estimate(self, lambda_opt, A, b, D, f):
128     # Calculate pos estimation given optimal lambda as eq. (23) in [2]
129
130     # Compute A^T A + D
131     ATA_plus_lambda_D = A.T @ A + lambda_opt * D
132

```



```

133     # Compute  $A^T b - f$ 
134     ATb_minus_lambda_f = A.T @ b - lambda_opt * f
135
136     # Compute  $\hat{y}() = (A^T A + D)^{-1} (A^T b - f)$ 
137     y_lambda = np.linalg.solve(ATA_plus_lambda_D, ATb_minus_lambda_f)
138
139     n = len(self.get_utm_coords()[0])
140     source_position = y_lambda[:n]
141
142     return source_position

```

330 9. Numerical Simulation

331 9.1. Simulation Setup

332 To evaluate the performance and robustness of the three acoustic localization algorithms (TDOA,
333 T-MM, and SR-LS), has been conducted extensive numerical simulations using the developed
334 framework. The simulation environment was configured as follows:

- 335 • **Geographic Area:** A region defined by coordinates [10-12° latitude, 83.5-85.5° longitude]
- 336 • **Bathymetry:** Realistic seabed topography data from the [General Bathymetric Chart of the](#)
337 [Oceans \(GEBCO\) database](#), loaded from a NetCDF file
- 338 • **Acoustic Propagation:** The Bellhop ray-tracing model was employed to simulate real-
339 istic underwater sound propagation, with 10 bathymetric points sampled between each
340 hydrophone-source pair to account for depth variations
- 341 • **Acoustic Error Modeling:** Six levels of TOA variance were tested [1.0e-5, 1.0e-4, 1.0e-3,
342 1.0e-2, 1.0e-1, 1.0], corresponding to progressively higher levels of measurement noise

343 9.2. Hydrophone Configuration

344 Four hydrophones were strategically positioned to form a square array:

- 345 • Hydrophone 1: (11.0, 84.0) at 20m depth
- 346 • Hydrophone 2: (11.03, 84.0) at 20m depth
- 347 • Hydrophone 3: (11.03, 84.03) at 20m depth
- 348 • Hydrophone 4: (11.0, 84.03) at 20m depth

349 The ambient noise level was set at 2.0 dB re 1 μ Pa; no random hydrophones were generated
350 for this simulation.

351 9.3. Target Configuration

352 The simulation included a single dark ship with the following parameters:

- 353 • Position: (11.032, 84.015)
- 354 • Speed: 10 knots
- 355 • Depth: 20 meters
- 356 • Heading: 180 degrees

357 9.4. Methodology

358 For each of the six TOA variance levels, has been conducted 100 independent simulation runs,
 359 recording the performance of each localization algorithm (TDOA, T-MM, and SR-LS) in terms of
 360 mean squared error (MSE) between the estimated and actual ship position. This approach allowed
 361 to systematically analyze how the performance of each algorithm degrades with increasing noise
 362 levels, providing insights into their robustness and suitability for different operational conditions.

363 9.5. Results and Analysis

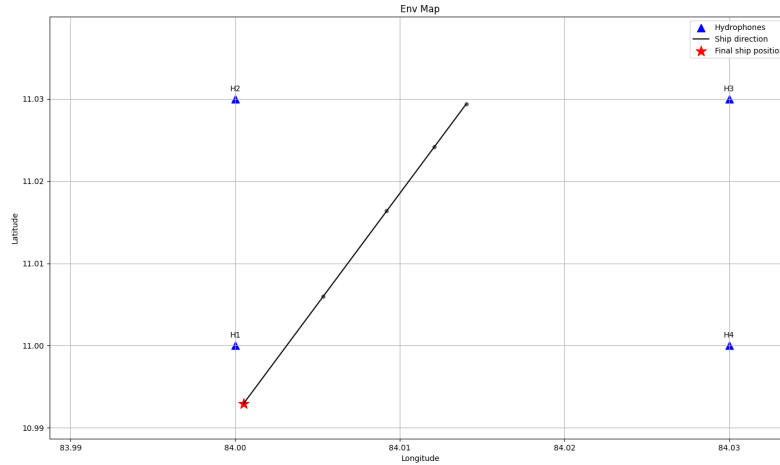


Fig. 2. Spatial configuration of the simulation showing the positions of the four hydrophones (blue markers) and the dark ship (red marker) in the defined geographic area.

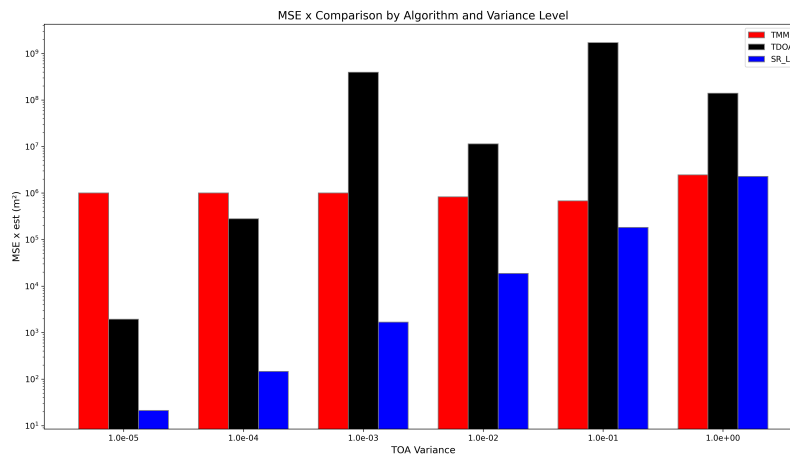


Fig. 3. Comparative Mean Square Error (MSE) of TDOA, T-MM, and SR-LS algorithms across different TOA variance levels.

364 Figure 4 shows the error progression as a function of increasing noise levels, providing insight
 365 into how rapidly each algorithm's performance degrades with higher measurement uncertainty.

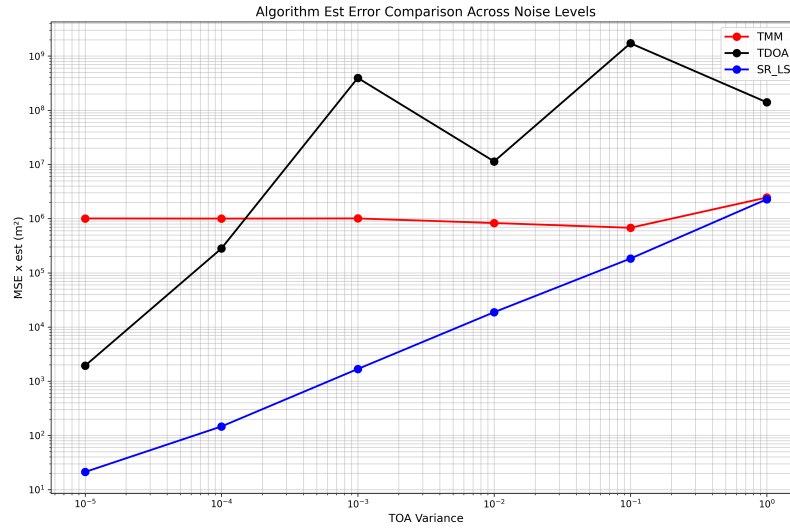


Fig. 4. Performance degradation trends of the three localization algorithms with increasing measurement noise. The logarithmic scale highlights the exponential relationship between noise levels and localization error.

The line chart format emphasizes the trend patterns and reveals critical threshold points where algorithm performance significantly deteriorates.

The results from the simulations demonstrate distinct performance characteristics for each algorithm:

- The conventional TDOA algorithm shows acceptable performance at lower noise levels (TOA variance $< 10^{-3}$) but degrades rapidly as noise increases, making it suitable only for relatively quiet underwater environments or scenarios with high-quality hydrophones.
- The T-MM algorithm exhibits significantly improved resilience to noise compared to standard TDOA. The majorization-minimization approach effectively mitigates the impact of measurement errors, demonstrating the value of this optimization technique.
- The SR-LS algorithm demonstrates the best overall robustness, particularly at higher noise levels. By formulating the problem in terms of squared ranges and employing global optimization techniques, this approach maintains acceptable localization accuracy even under challenging acoustic conditions where the other methods fail.

References

1. H. S. Shuangshuang Li and H. Esmail, "Underwater tdoa acoustical location based on majorization-minimization optimization," *Sensors* **20**, 4457 (2020).
2. A. Beck, P. Stoica, and J. Li, "Exact and approximate solutions of source localization problems," *IEEE Transactions on Signal Processing* **56**, 1770–1778 (2008).